Investigating the impact of regional transport on $PM_{2.5}$ formation using vertical observation during APEC 2014 Summit in Beijing

Yang Hua[1,2], Shuxiao Wang[1,2*], Jiandong Wang[1,2], Jingkun Jiang[1,2], Tianshu Zhang[3], Yu Song[4], Ling Kang[4], Wei Zhou[1,2], Runlong Cai[1,2], Di Wu[1,2], Siwei Fan[1,2], Tong Wang[1,2], Xiaoqing Tang[5], Qiang Wei[6], Feng Sun[6], Zhimei Xiao[7]

[1]State Key Joint Laboratory of Environment Simulation and Pollution Control, School of Environment, Tsinghua University, Beijing 100084, China.

[2]State Environmental Protection Key Laboratory of Sources and Control of Air Pollution Complex, Beijing 100084, China

[3]Anhui Institute of Optics and Fine Mechanics, Chinese Academy of Sciences, Hefei 230031, China

[4]College of Environmental Sciences and Engineering, Peking University, Beijing, 100871, China

[5] Hebei Environmental Monitoring Center, Hebei 050051, China

[6] Beijing Environmental Monitoring Center, Beijing 100048, China

[7] Tianjin Environmental Monitoring Center, Tianjin 300191, China

Corresponding to: Shuxiao Wang (shxwang@tsinghua.edu.cn)

ABSTRACT

During APEC (Asia-Pacific Economic Cooperation) Economic Leaders' 2014 Summit in Beijing, strict regional air emission control was implemented, providing a unique opportunity to investigate the transport and formation mechanism of fine particulate matter ($PM_{2.5}$). This study explores the use of vertical observation methods to investigate the influence of regional transport on $PM_{2.5}$ pollution in Beijing before and during the APEC Summit. Vertical profiles of extinction coefficient, wind, temperature and relative humidity were monitored at a rural site on the border of Beijing and Hebei Province. Three $PM_{2.5}$ pollution episodes were analysed. In episode 1 (October 27th to November 1st), regional transport accompanied with the accumulation of pollutants under unfavourable meteorological conditions led to the pollution. In episode 2 (November 2nd to 5th), pollutants left from episode 1 were retained in the boundary layer for 2 days in the region and then settled down to the surface, leading to an explosive increase of $PM_{2.5}$. The regional transport of aged aerosols played a crucial role in the heavy $PM_{2.5}$ pollution. In episode 3 (November 6th to 11th), emission from large point sources had been controlled for several days while primary emissions from diesel vehicle might lead to the pollution. It is found that ground-level observation of meteorology condition and air

quality could not fully explain the pollution process while vertical parameters (aerosol optical properties, winds, relatively humidity and temperature) improved the understanding of regional transport influence on heavy pollution process. Future studies may consider including vertical observations to aid investigation of pollutant transport especially during episodic events of rapidly increasing concentrations.

1. Introduction

With a rapid economic development and increases in energy consumption, large quantity of emissions has caused serious particulate matter pollution in China. Monitoring data show that Beijing-Tianjin-Hebei (BTH) region is one of the most polluted region in China (Zhao et al., 2013; Wang et al., 2014). The region was home to eight out of the top 10 most polluted Chinese cities in 2014 (MEP-Ministry of Environment Protection, 2015). In 2014, the annual average $PM_{2.5}$ (particulate matter with aerodynamic diameter less than 2.5 μm) concentration reached 95 $\mu g/m^3$ in the BTH region. With 21.5 million residents and 5.3 million vehicles, Beijing has been burdened with severe pollution episodes frequently in recent years (Beijing Municipal Bureau of Statistics, 2014). The capital is surrounded by mountains in three directions (north, west and east). The top three most polluted cities in China (Baoding, Xingtai and Shijiazhuang) are located in the south to Beijing. Polluted air mass from the south contributes to $PM_{2.5}$ pollution in Beijing (Wang et al., 2015). Source apportionment by Beijing Environmental Protection Bureau indicates regional transport contributed 28%-36% to $PM_{2.5}$ in Beijing in 2012-2013. During some severe pollution periods, regional contribution was more than 50% (http://www.bjepb.gov.cn/bjepb/413526/331443/331937/333896/396191/index.html). Quite a few researches have studied the causes of heavy polluted episodes in BTH region and show regional transport plays an important role in pollution formation. The sharp $PM_{2.5}$ build-up events in Beijing were unique while accumulation pollution process occurred at other cities in the region. This indicated that $PM_{2.5}$ was probably transported to Beijing from other cities (Zheng et al., 2015; Ji et al., 2014; Tao et al, 2014; Zhao et al., 2013). In the meanwhile, most severe pollutions are under stable synoptic meteorological conditions in Beijing (Sun et al., 2015; Zheng et al., 2015; Zhao et al., 2013). The low wind speed and stable synoptic meteorological condition at ground level cannot explain the reason that regional transport makes significant contribution to severe pollution. A previous study has shown the secondary aerosol in Beijing probably mainly formed over regional transport according to a vertical observation from the ground to 260m height. (Sun et al., 2015). Therefore, vertical profiles of meteorology and air quality might help us to understand the impacts of regional transport to heavy pollution during stagnant conditions.

As in other megacities with local sources and regional transport, air quality in Beijing are affected by many factors, including emissions inside the city, formation of secondary pollutants, atmospheric mixing, and regional transport. It has been well known that the strength of each factor varies according to emissions and/or weather conditions. Therefore, it is challenging to pin point the major contributors in any given time periods, either clean or polluted episodes. This is especially difficult in BTH region considering the complicated emission sources and transport processes.

Emission control measures implemented during some events provide a unique opportunity to investigate the impact of various factors influencing air quality. One of them was APEC (Asia-Pacific Economic Cooperation) Economic Leaders' 2014 Summit held in Beijing from November 5th to 11th, 2014. A strict emission pollution control plan was carried out in the BTH Region to improve air quality in Beijing from November 3rd to 11th for APEC. According to a conservative estimate by MEP, production of 9,289 plants were paused and 3900 plants were running at reduced capacity in six provinces (Beijing, Tianjin, Hebei, Shanxi, Shandong and Inner Mongolia); and more than 40 thousand construction sites were shut down temporally (http://www.zhb.gov.cn/gkml/hbb/qt/201411/t20141115_291482.htm). Other measures include traffic control (50% of private passenger vehicles and 70% of buses were off-road) and frequent road sweeping and cleaning in Beijing. More detail emission control measures are supplied in the supporting information. Studies have found that regional emission control effectively reduced air pollutant concentrations during the Summit (Wen et al., 2015; Tang et al., 2015; Han et al., 2015; Chen et al., 2015; Sun et al., 2016a). The significantly reduced local emissions led to reduced complexity of particulate matter pollution process, thus providing a unique opportunity to investigate the influence of transport events on $PM_{2.5}$ levels in Beijing.

The objective of the study is to investigate the impact of regional transport on $PM_{2.5}$ in Beijing using both ground-level and vertical observations. Field observation was conducted at a rural site (Liulihe) in southwest Beijing before and during the control period of the APEC 2014 Summit. Vertical profiles of temperature, RH (relative humidity), wind speed and direction, and extinction coefficient were observed as well as pollutants concentration and meteorological parameters on the ground. The characteristics of three $PM_{2.5}$ pollution episodes were analysed. Findings of this study will help explore vertical observation methods for in-depth analysis of the meteorological and transport influence. Furthermore, it can aid the development of future air quality management strategies in BTH and other regions around the globe, including emission control and air surveillance.

2. Field observation and analysis methods

2.1 Field observation site and sampling methods

Beijing is surrounded by mountains in the west, north and east directions, which blocks the pollutants from spreading. The open air corridor in the south exposes the capital to air mass passing Hebei Province (Fig. S1) a heavily polluted area in China. To investigate the impact of regional transport on Beijing, a rural site (Liulihe site, 116°2′E, 39°36′N) was chosen in the southwest of Beijing. It was located on the border of Beijing and Hebei Province (Fig. S1).

The field campaign was conducted from October 27th to November 12th, 2014, including both ground-level and vertical observations. Detailed information of instruments at Liulihe site is provided in Table S1. Ground-level observations included meteorological parameters, mass concentration of $PM_{2.5}$/PM_{10}, SO_2, NO_x and O_3 as well as physical and chemistry properties of PM. $PM_{2.5}$/PM_{10} mass concentration was determined by the TEOM method. Particle size distribution from 3nm to 10μm were measured by a spectrometer assembled in-house including one Nano scanning mobility particle sizers (NSMPS), one scanning mobility particle sizers (SMPS), and one aerodynamic particle sizer (APS) (Liu et al., 2014).

ACSM (Aerosol Chemical Speciation Monitor), a low-maintenance aerosol mass spectrometer, was used to measure non-refractory (NR) particulate matter with aerodynamic diameters smaller than 1μm (PM_1) (Ng et al., 2011). The ACSM data was calibrated with a collection efficiency (CE) value to compensate for the particle loss. The CE value of 0.45 recommended by Middlebrook et al. (2012) based on the monitoring site condition (see supporting information) was used in this study. The NR-PM_1 concentration measured by ACSM tracks well with $PM_{2.5}$ measured by the TEOM (R^2=0.91) and the regression slope is 0.43 (Fig. S2). Positive matrix factorization (PMF) with the PMF2.exe algorithm was used to distinguish different components of OA measured by ACSM (Paatero and Tapper, 1994). The PMF was performed and evaluated following the PMF analysis guide (http://cires1.colorado.edu/jimenez-group/wiki/index.php/PMF-AMS_Analysis_Guide). Three factors were distinguished (Fig. S3), i.e., HOA (hydrocarbon-like organic aerosol), SVOOA (semi volatile oxygenated organic aerosol) and LVOOA (low volatile oxygenated organic aerosol).

Beyond ground-level concentrations of routinely monitored air pollutants and meteorological parameters, the assessment was aided by vertical observations including vertical extinction coefficient profile, as well as vertical wind, RH and temperature profiles. The vertical extinction coefficient profiles depict the distribution of PM, which could be used to infer mixing process of particles transported in from high evaluations and those near the ground. Vertical wind profile indicate the transport direction. Vertical RH profiles reflect the strength of heterogeneous reaction at different layers. Vertical temperature profiles provide information on the stability of and mixing in the boundary layer. Lidar was used to observe the vertical optical properties of atmospheric aerosols at Liulihe site. The lidar consists of three parts, including emitting system, receiving system and signal analogue system (Chen et al., 2015). The laser source emitted pulse at 355/532nm. The pulse energy is 30MJ at 355nm and 20MJ at 532nm. The pulse repetition is 20Hz. The telescope for receiving system is based on a Cassegrain design. Diameter of the telescope is 200mm with a vertical resolution of 7.5m. The particle backscatter coefficient and extinction coefficient was retrieved by Fernald

method (Frederick et al., 1984). CFL-03 phased array wind profile radar was used to monitor the vertical wind speed and direction with resolutions of 50 m (0-1 km) and 100 m (1-5.5 km). Parameters of these instruments can be found in another paper (Wang et al., 2013). There are 300m blind area for CFL-03. Vertical profiles of atmospheric temperature and humidity were derived by profiling radiometers. The channel centre frequencies were 22-32 GHz (K-Band) and 51-59 GHz (V-Band). The vertical resolutions were 60 m (0-4 km) and 120 m (4-10 km).

2.2 Back trajectory analysis

Trajstat, a GIS-based software into which the HYSPLIT (Hybrid Single Particle Lagrangian Integrated Trajectory) model was loaded (Wang et al., 2009), was used to calculate the back trajectory. The model was run every 6 hours in a 24-hour mode back-trajectory mode at 1000 m above sea level from Liulihe site to identify the origins and path way of air mass. The meteorology data used in the mode was obtained from the Global Data Assimilation System (GDAS) model (http://www.ready.noaa.gov/READYamet.php).

2.3 Quantification of regional transport contribution

A novel technique was used to quantify the contribution of regional transport (Jia et al., 2008). The diurnal trend of $PM_{2.5}$ in Beijing often exhibit "Saw-tooth cycles" with a smoothly increasing or decreasing baseline upon which daily cycles are superimposed. Ancillary measurements around Beijing show that the baselines represent regional aerosols, while the daily cycles represent local aerosols. Following Jia et al. (2008), the total contribution is defined as the area under the concentration line (A_t), while its regional component is defined as the area under the baseline curve (A_r). Both areas are approximated using trapezoid numerical integration as Eq. (1):

$$A_N = \sum_{n=1}^{N-1} A_i = \sum_{n=1}^{N-1} \frac{(C_i + C_{i+1})}{2} \times (t_{i+1} - t_i) \quad (1)$$

Where N is the total number of hourly $PM_{2.5}$ concentrations in a specific time period, C_i is total concentration (for A_t) or baseline concentration (for A_r) value at time t_i (i=1, N-1). The baseline concentration curve is the line connecting daily afternoon minimal values. The percentage regional contribution (*R*) is expressed as following Eq. (2):

$$R = \frac{A_r}{A_t} \times 100\% \quad (2)$$

The uncertainty evaluation mainly includes systematic errors, random errors and sensitivities. The major systematic errors depend on the calibration of instruments for $PM_{2.5}$ concentration measurement. Minor systematic errors might be from the judging the location and height of the daily minima and the sensitivities analysis suggests these errors are less than 10%. Random errors include data measurement and quantification step, such as identifying the daily minima properly, dealing with days without less-obvious afternoon minima and using linear interpolation between the daily minima. All these errors are evaluate by Jia et al. (2008). As a whole, this technique has an uncertainty of 40%-50% for results of daily regional transport.

3. Results and discussion

3.1 General characteristics of atmospheric pollution before and during APEC summit

To investigate the changes in air quality during APEC summit, average pollutant concentrations and the rates of changes were calculated. Concentrations of $PM_{2.5}$, SO_2 and NO_2 decreased significantly during the emission control (November 3rd to November 12th) compared to the period before control (October 27th to November 2nd) as shown in Fig. S4 (a). The large rates of reduction were observed for NO_2 (37%) and SO_2 (36%), while the reduction in $PM_{2.5}$ was smaller (21%) but still significant (Fig. S4 (b)).

Three pollution episodes were selected to discuss the pollution characteristics during the observation (Fig. S5). Episode 1 (October 27th to November 1st) represents the period before the emission control. Episode 2 (November 2nd to 5th) was the first pollution episode during the emission control. Episode 3 (November 6th to 11th) was the second pollution episode during the emission control. $PM_{2.5}$ concentration at Miyun site (locate in northern Beijing, shown in Fig. S1, data source: Beijing EPB) is shown in Fig. S5 alongside Luilihe to demonstrate the synchronism of $PM_{2.5}$ levels at different sides in Beijing. At Luilihe, $PM_{2.5}$ concentration was the highest in episode 1 (140±70μg/m^3) before implementation of emission control, whereas the mean values were close during the last two episodes (91±75μg/m^3 and 89±61μg/m^3).

The average concentration of online non-refractory PM_1 chemical components was shown in Fig. 1. Average concentrations of OM (organic matter), NH_4^+, SO_4^{2-} and NO_3^- were the highest in episode 1 before emission control. During episode 2, those compounds decreased by 32-60%. In episode 3, the

average concentrations remained similar except NH_4^+ which decreased by 12%. HOA (related to primary emission), LVOOA and SVOOA were distinguished. Compared with episode1, the HOA, LVOOA and SVOOA decreased by 22%, 58% and 28% in episode 2. After that, LVOOA kept decreasing by 10% in episode 3 while HOA and SVOOA increased by 39% and 5%.

Overall, most meteorological parameters changed little during the three episodes except RH (Fig. S6)). The average ground-level RH (69%) in episode 1 was higher compared with those in episode 2 (50%) and in episode 3 (58%). Wind speed remained low during the entire observation. The average wind speed was 0.5m/s, 0.8m/s and 0.7m/s in episode 1, episode 2 and episode 3, respectively. The dominant wind direction was southwest during the 17 days observation. The frequency of southwest wind was above 60% during each of the three episodes, with the highest occurrence of 81% observed during episode 2.

The significant reduction in pollutant concentrations during APEC shown above implied that the emission control was effective. However, the general characteristics derived from ground-level observation are insufficient to identify the leading cause of particulate matter pollution, local emissions, regional transport, or both. Furthermore, the significant differences of particle chemical components changes from episode 2 to episode 3 under similar ground-level meteorological conditions and local emission intensity suggest different transport or formation mechanisms during those two episodes. Therefore, vertical observations will be used to aid further investigation in each of the three episodes in the following section.

3.2 Characteristics of heavy $PM_{2.5}$ pollution episodes and contribution of regional transport

3.2.1 Pollution process in episode 1

Episode 1 (October 27th to November 1st) was before emission control. The average concentration of $PM_{2.5}$ reached to 140μg/m^3. The high level of $PM_{2.5}$ is typical in Beijing during the autumn. There were two unique features in this episode. One is the continued increases of $PM_{2.5}$ mass and PM_1 component concentrations during the first four days, with OM showing a more distinct diurnal cycle (Fig. 2, Fig. 3 and Fig. S5). Another is the rapid increase of OM on Oct 29th (Fig. 3). Both suggest except secondary formation, other mechanisms might impact the OM growth and needs further investigation.

Various parameters collected during episode 1 are shown in Fig. 4. Combining the ground-level observation and vertical observation, it is evidenced that the pollution was caused by the regional

transport and pollutants accumulation later. Vertical extinction coefficient data observed at Yongledian site (116°47′E, 39°43′N) near Liulihe site were used (Fig. 4(a)), because the optical lidar at Liulihe didn't work in October. High level of PM appeared at approximately 2 km above ground (Fig. 4 (a)) and retained there for 1 day. The air mass came from the southwest where emissions were high (see horizontal wind direction profile, Fig. 4 (c)). Back trajectories also show air mass from southwest arrived in Liulihe, as well as Yongledian (Fig. S7). Then pollutants settled down (see downward vertical wind direction in Fig. 4 (b)) and mixed with aerosols on the ground (Fig. 4 (a)). The online particle size distribution also implied the transport process. During the same period (from 13:00 to 20:00 on October 28th), a new group of particles appeared and mixed with existing particles, indicating the arrival of aged aerosols (Fig. 4 (e)). As mentioned above, except secondary formation, other mechanisms might impact OM increase. The increase of OM might come from freshly-emitted organic particles and transported to the site instead of aged particles. One evidence is that both HOA and OOA increased significantly. Another is that the OM peak appeared after the transport occurrence, much earlier than SNA. It is noticed, even wind direction on the ground changed to north in the early morning on October 29th, it still retained in the southwest above 500m, indicating significant influence of regional transport.

In the next two days (October 30th to 31st), vertical wind direction was downward which was unfavorable for the pollutants diffusion (Fig. 5(a)). Weather Research & Forecasting Model (WRF) modeling results also show the whole region was under control of weak downward wind from late night on October 30th. (Fig. S8, modeling parameters are provided in supplemental information).What's more, both the atmosphere press and wind speed decreased at the same time (Fig. S6). This indicates the site was probably in the rear of cold anticyclone. The steady weather condition promote the pollutants accumulation. Meanwhile, high RH on the surface (Fig. S6) enhanced the formation of SA (secondary aerosol) as pointed out by Pathak et al. (2009). Under this condition, NH_4^+, SO_4^{2-} and NO_3^- concentrations increased at rates of 0.26μg/m^3/h, 0.21μg/m^3/h, and 0.58μg/m^3/h, respectively. The peak of NH_4^+, SO_4^{2-} and NO_3^- concentrations was two days later than OM. This also proved the organic particles were transported to Beijing and reached to the peak on October 29th and secondary formation became severe later, both of which promoted the pollution occurrence.

To quantify the impacts of regional transport, the transport component is calculated with the method introduced in section 2.2. The baseline needs to be defined first especially for pollution end timing. The vertical observation and ground observation were combined to discuss when the pollution ended (see supporting information). The regional component is calculated based on the determination of

baseline. For episode 1, the regional component accounted for 75% of $PM_{2.5}$ mass concentration observed at Liulihe site, indicating the important influence of regional transport on the pollution. It can be seen that episode 1 was a pollution episode influenced by transport process in Beijing. RH was high, wind speed was continuously low and wind direction was dominated by southwest in the surface. Vertical observation showed pollutants transported from southwest settled down. OM concentration increased significantly when the transport PM was observed. After that the low wind speed, high RH can easily promoted the pollutants accumulation and downward vertical wind was unfavorable for pollutants diffusion.

3.2.2 Pollution process in episode 2

Episode 2 (November 2nd to 5th) saw a lower mean $PM_{2.5}$ concentration (91±75μg/m^3) due to the implementation of emission control since November 2nd. Unlike the gradual accumulation of PM observed in episode 1, $PM_{2.5}$, OM and SNA had a sharp increase from November 4th to 5th. The concentrations of NH_4^+, SO_4^{2-} and NO_3^- increased at rates from the lowest to the highest of 0.88μg/m^3/h, 0.43μg/m^3/h, and 1.64μg/m^3/h, respectively, much faster than that in episode 1. OOA also increased much more significantly during this episode. The explosively increases of PM components mainly SA in such a short period of time is contrary to lower RH values in this episode leading to less heterogeneous reaction. Thus, such rapid increases in PM levels could be transport of aged aerosol from other regions, as hypothesized by previous studies where the transport process wasn't observed directly (Yue, et al., 2009; Massling., et al, 2009; Sun et al., 2014; Sun et al., 2016b).

With the aid of vertical observation, an in-depth investigation revealed atmospheric processes leading to the peak concentrations during November 4th to 5th. Firstly, after the end of episode 1 at November 1st, relatively high PM levels still resided at 1000m (from November 2nd to 3rd) as shown in the vertical extinction coefficient (Fig. 7). Furthermore, a band of high PM centered around 750 m were observed ((Fig. S9) on November 3rd at another site (Baoding site, 115°31′E, 38°52′N, shown in Fig. S1) in the BTH region, suggesting a wide-spread PM aloft in the region. During the next two days, the pollutants were transported in the region and the slow winds (average speed of 4.8m/s at 1000 m) allowed aerosols ample time to age in their journey. Back trajectories showed transport of air mass from the southwest at the night of November 3rd (Fig. S10), consistent with the vertical wind profile observed at Liulihe (Fig.5 (b) and Fig.9). On November 3rd and November 4th, the downward motion of air mass around 1000 m above ground intensified, bringing the aged aerosols down and mixing them with the aerosols on the ground. The well mixed boundary layer with regard to aerosol is evidence in Fig. 8 with a fairly uniform distribution from the ground to 900 m. Consequently,

secondary chemical component concentrations of PM_1 (Fig. 2 and Fig. 3) started ascending with remarkably fast rates.

Dry and clean air mass from the north arrived in the early morning on November 5th. RH started to increase significantly at 10:00 and wind speed became higher from 12:00. At the same time, $PM_{2.5}$ concentration started to decrease. Based on the analysis, the pollution ended up at 12:00. The calculation shows regional transport contributed 62%, relatively lower than that during episode 1 (Fig. 6).

Rather than chemical reaction, aged aerosols settled down and had important contribution to the high $PM_{2.5}$ concentration in episode 2. Vertical observations found that the aged aerosol settled down and caused the explosive increase of SNA in such a short time, which can't be explained by the ground-level observations. It was also noticed that the high $PM_{2.5}$ level appeared when the emission control just started, which means this episode was partly caused by regional transport before control. Even when local emission control was conducted effectively, the uncontrolled regional emission still led to severe particulate matter pollution in Beijing.

3.2.3 Pollution process in episode 3

During episode 3 (November 6th to 11th), Luilihe site recorded a relatively high average $PM_{2.5}$ concentration of 89±61μg/m^3. Furthermore, this episode is characterized by much more and faster increases in OM concentrations than SNA (Fig. 2 and Fig. 3). Specifically, concentrations of aerosol related with fuel combustion (HOA) increased significantly. While SNA increased slowly (NH_4^+ and NO_3^-) or changed little (SO_4^{2-}). All of these indicate primary emission rather than the formation of SA was the dominant cause.

Vertical extinction coefficient shows pollutants appeared at 2000-2500m on November 7th. The air mass came from the northwest and the vertical convection bringing them down on November 7th and 8th (Fig. 7, Fig. 5(b) and Fig. 9). Air mass trajectories at 1000 m also show air mass arrived in Beijing from the south on November 7th but changing to the northwest on November 8th (Fig. S11). Because the northwest was less polluted and the effective emission control in BJH region during the APEC, the regional transport of PM was weakened. This is supported by an estimated regional contribution of 53% to $PM_{2.5}$ in Beijing, much lower than in episode 1 (75%) and episode 2 (63%).

Figure 10 depicts black carbon (BC) concentrations measured by Aethalometer and OM concentrations measured by ACSM. They tracked each other well during this episode. Concentrations

of BC, a marker of vehicular emission in urban settings, had two peaks every day. One was in the early morning and another was after morning rush hour of 10:00-11:00 am. The first peak might result from diesel vehicle emissions (Westerdahl, et al., 2009). This is because transportation of goods to Beijing via heavy-duty diesel vehicles has been permitted at night only, and the number of trucks was large. The second peak might be resulted from vehicles from outside coming into Beijing. Vehicles not registered in Beijing are banned to come into Beijing in the rush hour (7:00 am to 9:00 am), which reduces the morning peaks and smoothes the traffic flow. The vehicles coming into Beijing reach a peak after morning rush hour (http://wenku.baidu.com/link?url=SjtPVT1tgo4ON0KDQ5py8ehw1ZAzUr3k0mSd74D3F-8lOQZPPvedZiro6E5-MOeFFuww7VZjy3XwRqfU-mHXkg0_8kSy5p9FGyokfrFZX0e). As a result, a second peak appeared in the late morning at Liulihe site where is close the entrance from Hebei Province into Beijing. When the regional emission control was conducted effectively and air mass was from relatively clean areas, traffic emissions in and around the city became the dominant source.

4. Conclusion

This study indicates that the meteorology condition on the ground sometime couldn't explain the air pollution process, especially the air pollutions episodes significantly impacted by regional transport of air pollutants. Vertical observation can provide the vertical meteorological and optical profile, which can help identify the regional transport episodes. Combining the ground-level observation with information from radars, we can determine the regional transport influence on air quality.

Three episodes of different types under similar ground meteorological condition were discussed in this study. In episode 1, particle concentration accumulated under the unfavorable meteorological condition after transport occurred. The transport pollutants brought organic aerosol and SNA increased under high RH later. In episode 2, pollutants left from episode 1 was retained in the boundary layer in the region. When vertical wind direction changed to downward, the pollutants were settled down. As a result, OM and SNA increased much explosively. In episode 3, when the control had been conducted for several days, SNA and OA concentration increased much less while HOA and increased significantly. The pollution might be caused by the primary emission from diesel vehicles.

Our research suggests regional transport of air pollutants has significant contribution (up to 70%) to severe secondary particle pollution, even when local emission was controlled effectively (53%, such as in APEC summit). Although lots of efforts were paid to air quality management in Beijing, the

equal efforts need to be paid to regional emission to ensure the clean air. What's more, diesel vehicle emission at night in Beijing might be an important pollution source and needs further investigation.

Acknowledgements

This work was supported by the MEP's Special Funds for Research on Public Welfare (201409002), Strategic Priority Research Program of the Chinese Academy of Sciences (XDB05020300), and National Natural Science Foundation of China (21521064). The authors also appreciate the support from Collaborative Innovation Centre for Regional Environmental Quality.

References

Beijing Municipal Bureau of Statistics, The national statistical yearbook of China in 2014, 2015.

Chen, C., Sun, Y., Xu, W., Du, W., Zhou, L., Han, T., Wang, Q., Fu, P., Wang, Z. and Gao, Z. (2015) Characteristics and sources of submicron aerosols above the urban canopy (260 m) in Beijing, China, during the 2014 APEC summit. Atmos. Chem. Phys 15(22), 12,879-812,895.

Chen, Z., Zhang, J., Zhang, T., Liu, W. and Liu, J. (2015) Haze observations by simultaneous lidar and WPS in Beijing before and during APEC, 2014. Science China Chemistry 58(9), 1385-1392.

Frederick G. Fernald. (1984) Analysis of atmospheric lidar observation: some comments. Applied Optics 84(23), 652-653.

Han, T., Xu, W., Chen, C., Liu, X., Wang, Q., Li, J., Zhao, X., Du, W., Wang, Z. and Sun, Y. (2015) Chemical apportionment of aerosol optical properties during the Asia‐Pacific Economic Cooperation (APEC) summit in Beijing, China. Journal of Geophysical Research: Atmospheres 120(23), 12281-12295.

Ji, D., Li, L., Wang, Y., Zhang, J., Cheng, M., Sun, Y., Liu, Z., Wang, L., Tang, G., Hu, B., Chao, N., Wen, T. and Miao, H. (2014) The heaviest particulate air-pollution episodes occurred in northern China in January, 2013: Insights gained from observation. Atmospheric Environment 14(92), 546-556.

Jia, Y., Rahn, K.A., He, K., Wen, T. and Wang, Y. (2008) A novel technique for quantifying the regional component of urban aerosol solely from its sawtooth cycles. Journal of Geophysical Research: Atmospheres 113(D21).

Liu, J., Jiang, J., Zhang, Q., Deng, J. and Hao, J. (2014) A spectrometer for measuring particle size distributions in the range of 3 nm to 10 μm. Frontiers of Environmental Science & Engineering 16(10), 63-72.

Massling, A., Stock, M., Wehner, B., Wu, Z., Hu, M., Brüggemann, E., Gnauk, T., Herrmann, H. and Wiedensohler, A. (2009) Size segregated water uptake of the urban submicrometer aerosol in Beijing. Atmospheric Environment 43(8), 1578-1589.

Middlebrook, A.M., Bahreini, R., Jimenez, J.L. and Canagaratna, M.R. (2012) Evaluation of composition-dependent collection efficiencies for the aerodyne aerosol mass spectrometer using field data. Aerosol Science and Technology 46(3), 258-271.

Ng, N.L., Herndon, S.C., Trimborn, A., Canagaratna, M.R., Croteau, P.L., Onasch, T.B., Sueper, D., Worsnop, D.R., Zhang, Q., Sun, Y.L. and Jayne, J.T. (2011) An Aerosol Chemical Speciation Monitor (ACSM) for Routine Monitoring of the Composition and Mass Concentrations of Ambient Aerosol. Aerosol Science and Technology 45(7), 780-794.

Paatero, P. and Tapper, U. (1994) Positive matrix factorization: A non‐negative factor model with optimal utilization of error estimates of data values. Environmetrics 5(2), 111-126.

Pathak, R.K., Wu, W.S. and Wang, T. (2009) Summertime $PM_{2.5}$ ionic species in four major cities of China: nitrate formation in an ammonia-deficient atmosphere. Atmospheric Chemistry and Physics, 9(5), 1711-1722.

Tang, G., Zhu, X., Hu, B., Xin, J., Wang, L., Münkel, C., Mao, G. and Wang, Y. (2015) Impact of emission controls on air quality in Beijing during APEC 2014: lidar ceilometer observations. Atmospheric Chemistry and Physics 15(21), 12667-12680.

Sun, Y., Jiang, Q., Wang, Z., Fu, P., Li, J., Yang, T. and Yin, Y. (2014) Investigation of the sources and evolution processes of severe haze pollution in Beijing in January 2013. Journal of Geophysical Research: Atmospheres 119(7), 4380-4398.

Sun, Y., Du, W., Wang, Q., Zhang, Q., Chen, C., Chen, Y., Chen, Z., Fu, P., Wang, Z. and Gao, Z. (2015) Real-Time Characterization of Aerosol Particle Composition above the Urban Canopy in Beijing: Insights into the Interactions between the Atmospheric Boundary Layer and Aerosol Chemistry. Environmental Science & Technology 49(19), 11340-11347.

Sun, Y., Wang, Z., Wild, O., Xu, W., Chen, C., Fu, P., Du, W., Zhou, L., Zhang, Q. and Han, T. (2016a) "APEC Blue": Secondary Aerosol Reductions from Emission Controls in Beijing. Scientific reports 6, 20668.

Sun, Y., Chen, C., Zhang, Y., Xu, W., Zhou, L., Cheng, X., Zheng, H., Ji, D., Li, J. and Tang, X. (2016b) Rapid formation and evolution of an extreme haze episode in Northern China during winter 2015. Scientific reports 6, 27151.

Tang, G., Zhu, X., Hu, B., Xin, J., Wang, L., Münkel, C., Mao, G. and Wang, Y. (2015) Impact of emission controls on air quality in Beijing during APEC 2014: lidar ceilometer observations. Atmospheric Chemistry and Physics 15(21), 12667-12680.

Tao, M., Chen, L., Xiong, X., Zhang, M., Ma, P., Tao, J. and Wang, Z. (2014) Formation process of the widespread extreme haze pollution over northern China in January 2013: Implications for regional air quality and climate. Atmospheric Environment 98, 417-425.

Wang, J., Wang, S., Jiang, J., Ding, A., Zheng, M., Zhao, B., Wong, D.C., Zhou, W., Zheng, G. and Wang, L. (2014) Impact of aerosol–meteorology interactions on fine particle pollution during China's severe haze episode in January 2013. Environmental Research Letters 9(9), 094002.

Wang, L., Liu, Z., Sun, Y., Ji, D. and Wang, Y. (2015) Long-range transport and regional sources of $PM_{2.5}$ in Beijing based on long-term observations from 2005 to 2010. Atmospheric Research 157, 37-48.

Wang, M., Wei, W., Ruan, Z., He, Q. and Ge, R. (2013) Application of wind-profiling radar data to the analysis of dust weather in the Taklimakan Desert. Environmental monitoring and assessment 185(6), 4819-4834.

Wang, Y., Zhang, X. and Draxler, R.R. (2009) TrajStat: GIS-based software that uses various trajectory statistical analysis methods to identify potential sources from long-term air pollution measurement data. Environmental Modelling & Software 24(8), 938-939.

Wen, W., Cheng, S., Chen, X., Wang, G., Li, S., Wang, X. and Liu, X. (2015) Impact of emission control on $PM_{2.5}$ and the chemical composition change in Beijing-Tianjin-Hebei during the APEC summit 2014. Environmental science and pollution research 23(5) 4509-4521.

Westerdahl, D., Wang, X., Pan, X. and Zhang, K.M. (2009) Characterization of on-road vehicle emission factors and microenvironmental air quality in Beijing, China. Atmospheric Environment 43(3), 697-705.

Yue, D., Hu, M., Wu, Z., Wang, Z., Guo, S., Wehner, B., Nowak, A., Achtert, P., Wiedensohler, A. and Jung, J. (2009) Characteristics of aerosol size distributions and new particle formation in the summer in Beijing. Journal of Geophysical Research: Atmospheres 114(D2).

Zhang, Z.Y., Wong, M.S. and Lee, K.H. (2015) Estimation of potential source regions of $PM_{2.5}$ in Beijing using backward trajectories. Atmospheric Pollution Research 6(1), 173-177.

Zhao, B., Wang, S., Dong, X., Wang, J., Duan, L., Fu, X., Hao, J. and Fu, J. (2013) Environmental effects of the recent emission changes in China: implications for particulate matter pollution and soil acidification. Environmental Research Letters 8(2), 024031.

Zhao, X., Zhao, P., Xu, J., Meng, W., Pu, W., Dong, F., He, D. and Shi, Q. (2013) Analysis of a winter regional haze event and its formation mechanism in the North China Plain. Atmospheric Chemistry and Physics 13(11), 5685-5696.

Zheng, G.J., Duan, F.K., Su, H., Ma, Y.L., Cheng, Y., Zheng, B., Zhang, Q., Huang, T., Kimoto, T., Chang, D., Poeschl, U., Cheng, Y.F. and He, K.B. (2015) Exploring the severe winter haze in Beijing: the impact of synoptic weather, regional transport and heterogeneous reactions. Atmospheric Chemistry and Physics 15(6), 2969-2983.

Figures

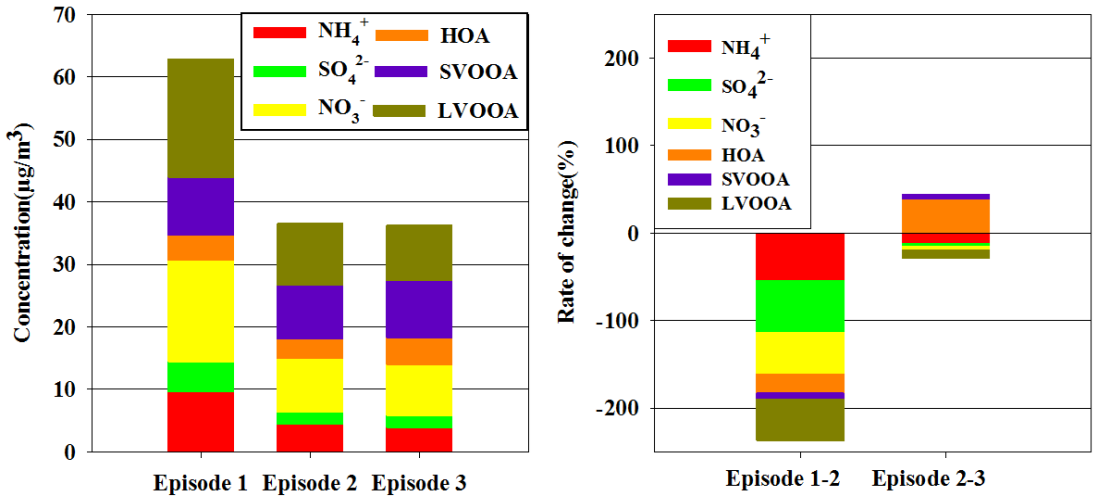

Figure 1. Non-refractory PM_1 chemical components at Liulihe site in the three episodes (a) average non-refractory PM_1 chemical components; (b) differences of chemical components among episodes

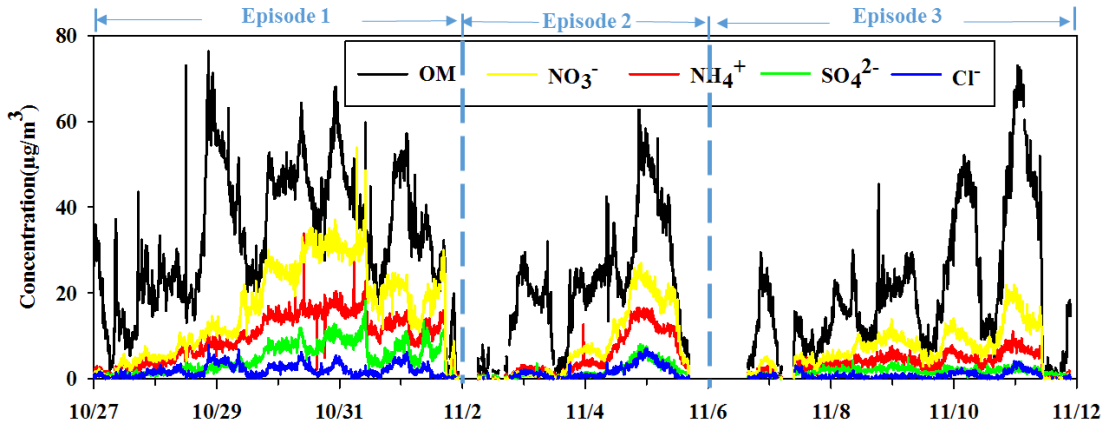

Figure 2. Temporal changes of non-refractory PM_1 chemical components at Liulihe site

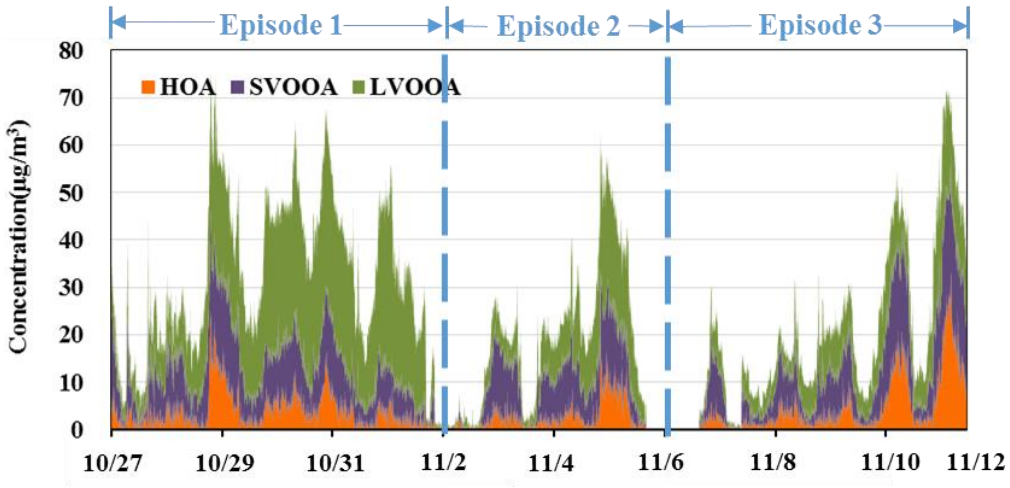

Figure 3. The temporal changes of organic components in PM_1 at Liulihe site

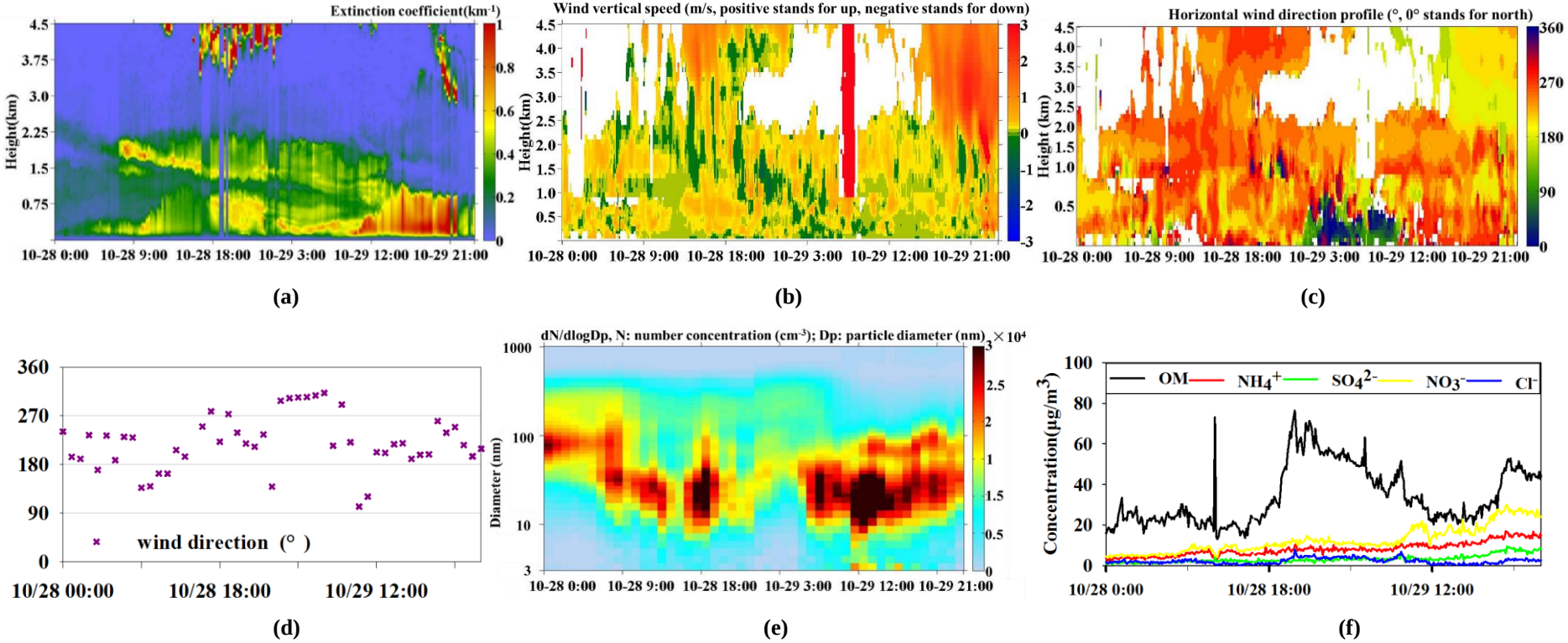

Figure 4. Characteristics of particulate matters and meteorological parameters during episode 1

(a) Vertical profile of extinction coefficient (Yongledian site);(b) Vertical profile of wind vertical direction and speed; (c) Horizontal wind direction profile; (d) wind direction on the ground; (e) Particle size distribution; (f) NR-PM_1 chemical components

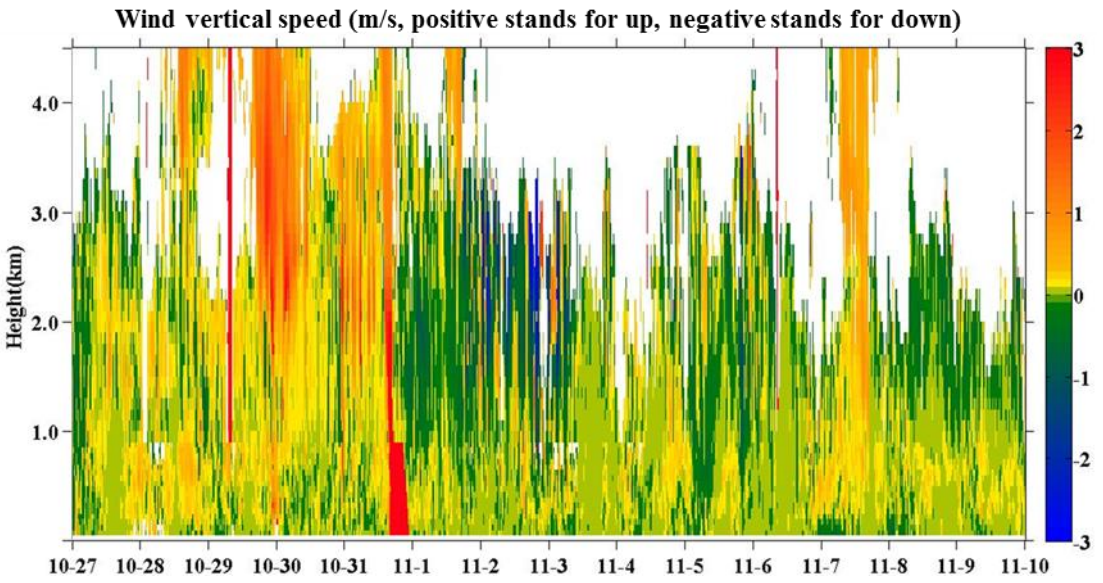

(a)

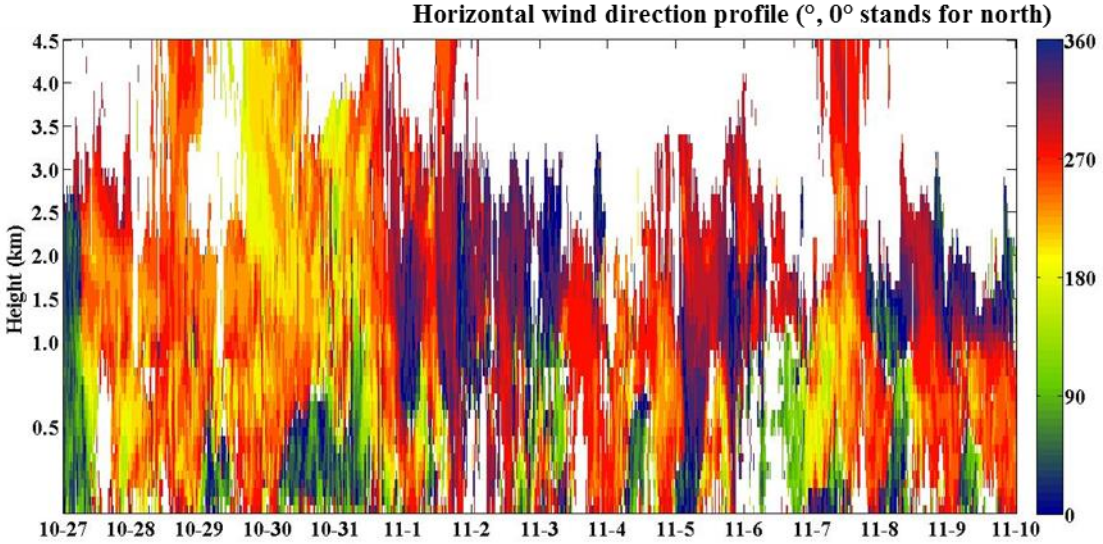

(b)

Figure 5. Vertical profile of wind at Liulihe site

(a) Wind vertical speed; (b) Wind horizontal direction profile

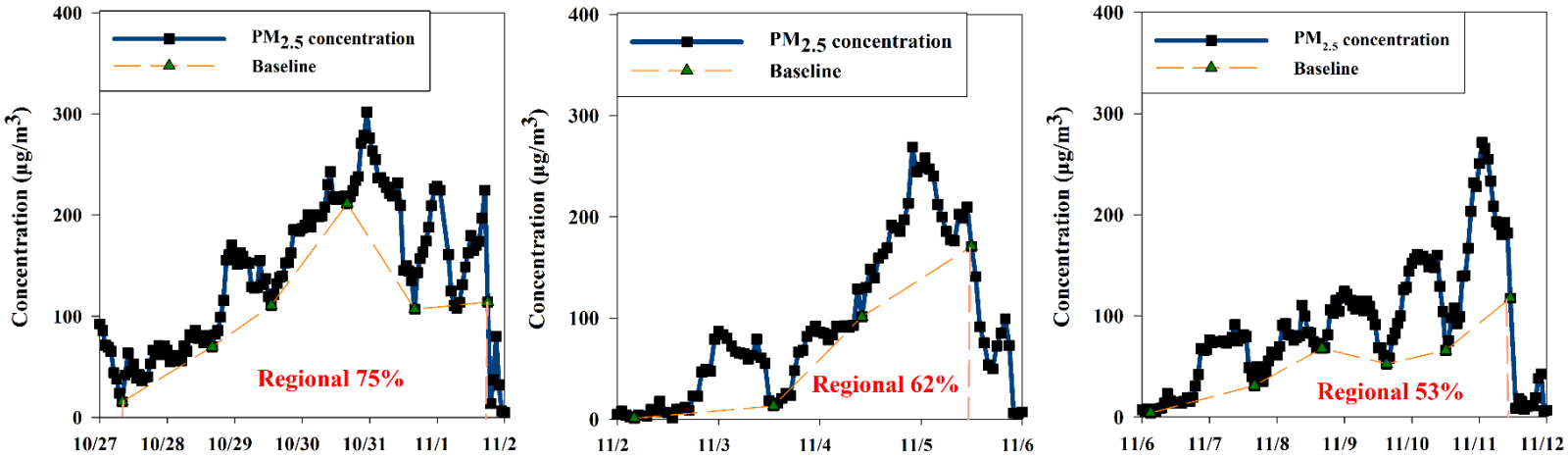

Figure 6. Regional and local components of the three episodes at Liulihe site

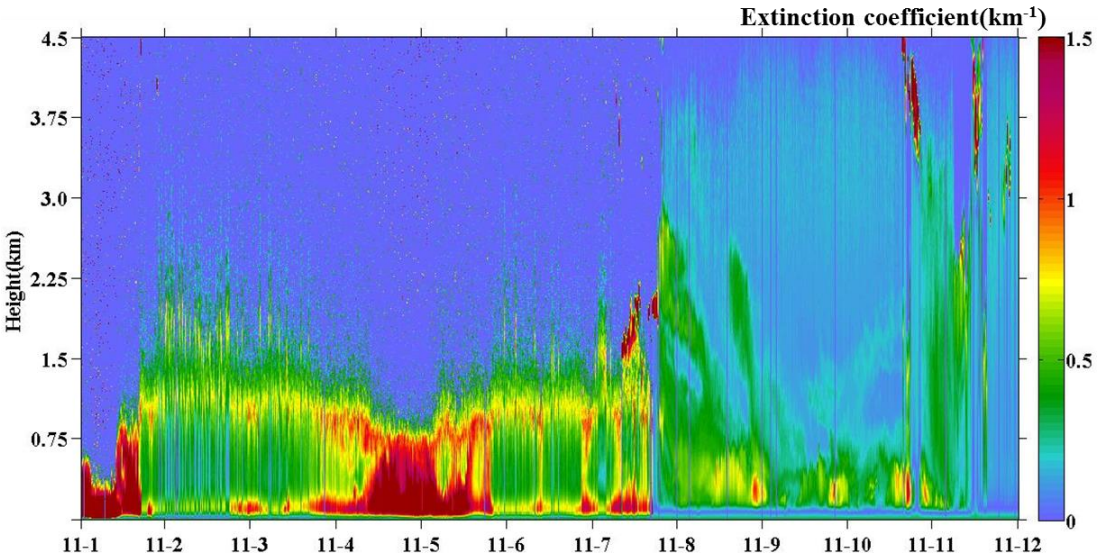

Figure 7. Vertical profile of extinction coefficient at Liulihe site

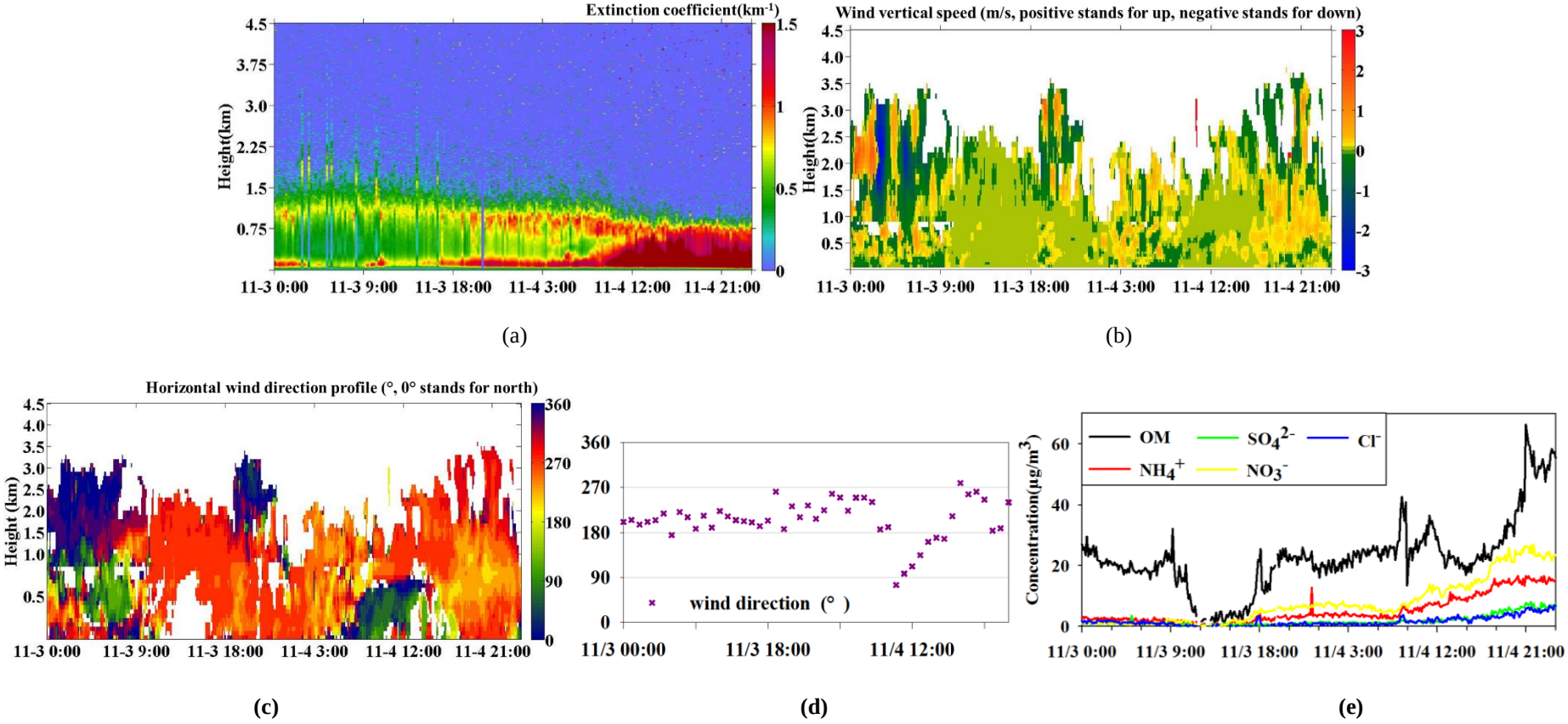

Figure 8. Characteristics of particulate matters and meteorological parameters during episode 2

(a) Vertical profile of extinction coefficient;(b) Vertical profile of wind vertical direction and speed; (c) Horizontal wind direction profile; (d) wind direction on the ground; (e) NR-PM$_1$ chemical components

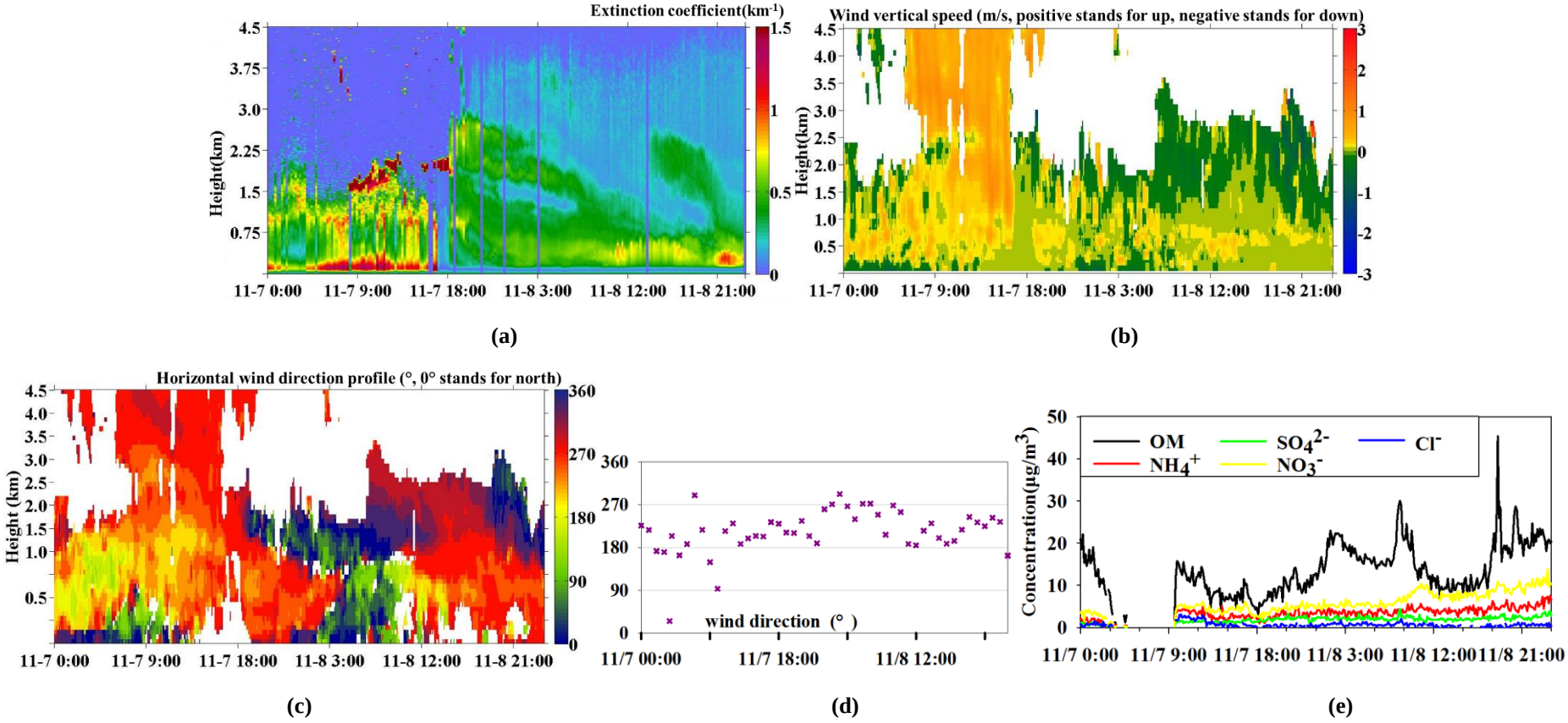

Figure 9. Characteristics of particulate matters and meteorological parameters at Liulihe site during episode 3

(a) Vertical profile of extinction coefficient;(b) Vertical profile of wind vertical direction and speed; (c) Horizontal wind direction profile; (d) wind direction on the ground; (e) NR-PM$_1$ chemical components

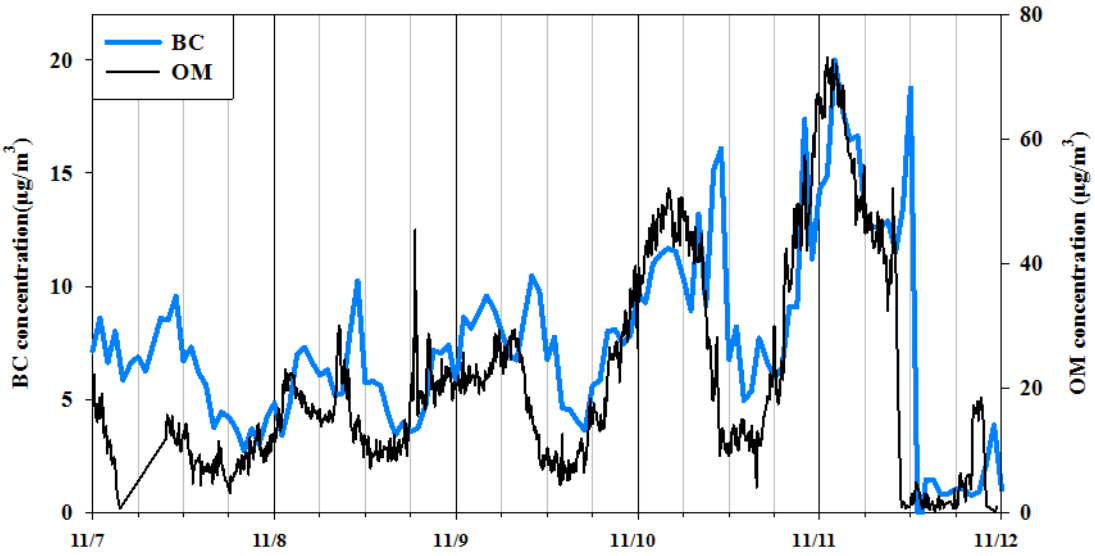

Figure 11. BC and OM concentrations of PM_1 at Liulihe site during episode 3